

Electronic Supplementary Information

[NH₃(CH₂)₄NH₃]SnX₄ (X = Br, I): Dion-Jacobson type 2-D Perovskites with Short Interlayer Spacing

Nagale S. Vishwajith,^a Mridul Krishna Sharma,^{a†} Isha Jain,^{a†} Pratap Vishnoi^{a*}

† MKS and IJ contributed equally.

New Chemistry Unit, International Centre for Materials Science
Jawaharlal Nehru Centre for Advanced Scientific Research,
Jakkur P. O., Bangalore-560064, India
E-mail: pvishnoi@jncasr.ac.in

Content Table	Page
Materials	S3
Synthesis of (1,4-BDA)SnBr ₆ , (1,4-BDA)SnBr ₄ , (1,4-BDA)SnI ₄	S3
Single crystal X-ray diffraction	S4
Powder X-ray diffraction	S4
UV-visible spectroscopic studies	S4
X-ray photoelectron spectroscopy (XPS)	S4
Field emission scanning electron microscopy (FESEM) and energy dispersive spectrometry (EDS) mapping	S4
Photoluminescence spectroscopy	S4
Thermogravimetric analysis (TGA)	S4
Differential scanning calorimetry (DSC)	S4
Table S1. Comparison of reported Dion-Jacobson type A ₂ SnBr ₄ and A ₂ SnI ₄ 2D compounds	S5
Table S2. Single crystal data and structure refinement details of (1,4-BDA)SnBr ₆	S5
Table S3. Single crystal data and structure refinement details of (1,4-BDA)SnBr ₄	S6
Table S4. Single crystal data and structure refinement details of (1,4-BDA)SnI ₄	S7
Table S5. Bond distances & bond angles as obtained from the SCXRD data of the compounds reported in this study	S8
Fig. S1. Simulated and experimental powder X-ray diffraction patterns of (1,4-BDA)SnBr ₄	S9
Fig. S2. Simulated and experimental powder X-ray diffraction patterns of (1,4-BDA)SnI ₄	S10
Fig. S3. Single-crystal structure of (1,4-BDA)SnBr ₆	S10
Fig. S4. (a) and (b) are ball and stick models of the (1,4-BDA)SnBr ₄ and (1,4-BDA)SnI ₄ perovskite layers.	S11
Fig. S5. Orientation of BDA in three different structures reported in this study.	S11
Table S6. Elemental ratio (atomic %) obtained from the EDS spectra.	S11
Fig. S6. Energy-dispersive X-ray spectra of (a) (1,4-BDA)SnBr ₄ and (b) (1,4-BDA)SnI ₄ .	S12
Fig. S7. XPS survey spectra of (a) (1,4-BDA)SnBr ₄ and (b) (1,4-BDA)SnI ₄ .	S13
Fig. S8. Core level XPS spectra of (1,4-BDA)SnBr ₄ (a) Nitrogen and (b) Carbon & (1,4-BDA)SnI ₄ (c) Nitrogen and (d) Carbon.	S13
Fig. S9. PXRD comparing the ambient stabilities of (1,4-BDA)SnBr ₄	S14
Fig. S10. PXRD comparing the ambient stabilities of (1,4-BDA)SnI ₄	S15
Fig. S11. TGA curves of (a) (1,4-BDA)SnBr ₄ and (b) (1,4-BDA)SnI ₄	S15
Fig. S12. DSC plots of (a) (1,4-BDA)SnBr ₄ and (b) (1,4-BDA)SnI ₄	S16
Fig. S13. Tauc plot for (1,4-BDA)SnBr ₆	S16
Fig. S14. Tauc plot for (1,4-BDA)SnBr ₄	S17
Fig. S15. Tauc plot for (1,4-BDA)SnI ₄	S17
References	S18

Experimental Section

Materials. 1,4-Butanediamine (Sigma Aldrich, 99%), Tin metal (Sigma Aldrich, <150 μm particle size, 99.5% trace metal basis), 48 wt.% HBr in H_2O (Merck, India), 57 wt.% HI in H_2O (Merck, India) and 50 wt.% H_3PO_2 in H_2O were purchased from commercial sources. All the compounds reported here were synthesised hydrothermally as single crystalline materials and structurally characterized from single crystal X-ray diffraction data.

Synthesis of (1,4BDA)SnBr₆. 1,4-Butanediamine (87.70 mg, 101 μL , 1.0 mmol) was added to a 23 mL Teflon vial containing Sn (118 mg, 1.0 mmol), (3mL) of 48 wt.% aqueous HBr and (110 μL , 2.0 mmol) of H_3PO_2 50 wt.% in H_2O . The Teflon vial was kept in a stainless-steel autoclave and heated in an oven at 160 $^\circ\text{C}$ for 24 hours. The reaction was cooled to room temperature at a cooling rate of 0.5 $^\circ\text{C}/\text{min}$, yielding yellow crystals. The yellow crystals of (1,4-BDA)SnBr₆ were rapidly filtered out of the mother liquor, pressed with Whatman filter paper, and dried in a vacuum oven.

Synthesis of (1,4-BDA)SnBr₄. 1,4-Butanediamine (87.70 mg, 101 μL , 1.0 mmol) was added to a 23 mL Teflon vial containing Sn (118.0 mg, 1.0 mmol), (452 μL , 4.0 mmol) of 48 wt.% aqueous HBr and 2 mL of H_3PO_2 50 wt.% in H_2O . The Teflon vial was kept in a stainless-steel autoclave and heated in an oven at 200 $^\circ\text{C}$ for 2 hours. The reaction was cooled to room temperature by switching off the oven, and the Teflon vial was opened after 12 hours, which yielded yellow crystals. The yellow crystals of (1,4-BDA)SnBr₄ were rapidly filtered out of the mother liquor, pressed with Whatman filter paper, and dried in a vacuum oven.

Synthesis of (1,4-BDA)SnI₄. 1,4-Butanediamine (87.70 mg, 101 μL , 1.0 mmol) was added to a 23 mL Teflon vial containing Sn metal (118.0 mg, 1.0 mmol), (530 μL , 4.0 mmol) of 57 wt.% aqueous HI, and 2mL of H_3PO_2 50 wt.% in H_2O . The Teflon vial was kept in a stainless-steel autoclave and heated in an oven at 200 $^\circ\text{C}$ for 2 hours. The reaction was cooled to room temperature by switching off the oven, and the Teflon vial was opened after 12 hours, which yielded red crystals. The red crystals of (1,4-BDA)SnI₄ were rapidly filtered out of the mother liquor, pressed with Whatman filter paper, and dried in a vacuum oven.

Single crystal X-ray diffraction. Single crystals of each sample were mounted on a quartz fibre with the help of silicon grease on a Bruker D8 Venture diffractometer equipped with photon detector and graphite-monochromatic Mo-K α X-ray source (wavelength = 0.71073 \AA). Data were integrated by using APEX-3 software. XPREP was used to check for the possibility

of higher symmetry. The data were solved and refined by using SHELX 14.0^{S1} and Olex2.^{S2} All non-hydrogen atoms were refined anisotropically. The crystal structure figures were drawn by using VESTA 3.5.7.^{S3}

Powder X-ray diffraction. Crystals were powdered in mortar and pestle before being placed in a PXRD sample holder. The PXRD data were collected on a Rigaku Smart Lab diffractometer equipped with a Cu-K α X-ray source (wavelength = 1.54059 Å).

UV-visible spectroscopic studies. Agilent Cary 5000 UV-VIS-NIR spectrophotometer instrument was used in reflectance mode, and reflectance in the range of 250-800 nm was obtained to determine the band gap.

X-ray photoelectron spectroscopy (XPS). The XPS data of the samples was collected on a Thermo Scientific K-Alpha X-ray photoelectron spectrometer equipped with a monochromatic, micro-focused, low-power Mg-K α X-ray source. The samples were powdered and then mounted on the XPS sample holder using double-sided copper tape. Survey scan spectra were measured in the 10 eV-1000 eV range, and core-level spectra were recorded for each sample.

Field emission scanning electron microscopy (FESEM) and energy dispersive spectrometry (EDS) mapping. FESEM images were collected ZEISS Gemini SEM – Field Emission Scanning Electron Microscope and Energy Dispersive Spectrometry (EDS) images were collected on OXFORD ULTIM MAX-40.

Photoluminescence spectroscopy. Photoluminescence spectrum was measured on FLS1000 Spectrometer of Edinburgh Instruments, equipped with 450 W ozone free Xenon arc lamp as the excitation source and visible PMT 900 (250 nm – 900 nm) detector.

Thermogravimetric analysis (TGA). The TGA data of all the compounds were collected under an inert nitrogen atmosphere on a Mettler Toledo TGA 1 STAR^e instrument.

Differential scanning calorimetry (DSC). Mettler Toledo DSC 3 STAR^e calorimeter was used to collect DSC with a 10 K/min ramp rate in a nitrogen atmosphere.

Table S1. Comparison of reported Dion-Jacobson type 2D A'SnBr₄ and A'SnI₄ perovskites.^a

Compound	Δd	σ^2	Interlayer Spacing (Å)	Experimental Bandgap (eV)	Ref
(1,8-ODA)SnBr ₄	8.18 x 10 ⁻⁵	3.69	13.426	Not available	S4

(1,4-BDA)SnBr ₄	4.462 x 10 ⁻³	18.6252	9.549	2.64	This work
[C ₅ H ₁₁ N(CH ₂) ₂ NH ₃]SnI ₄	3.16 X 10 ⁻³	26.29	10.364	Not available	S5
[NH ₃ (CH ₂) ₅ NH ₃]SnI ₄	2.82 X 10 ⁻⁴	2.416	10.216	Not available	S5
[C ₃ H ₄ N ₂ (CH ₂) ₂ NH ₃]SnI ₄	1.15 X 10 ⁻³	9.649	10.022	1.67	S6
[(CH ₃) ₃ N(CH ₂) ₂ NH ₃]SnI ₄	2.704 x 10 ⁻⁵	2.12	10.129	1.97	S7
[(C ₃ H ₆ N ₂) ₂]SnI ₄	6.32 X 10 ⁻³	22.90	9.492	Not available	S8
[C ₈ H ₈ N ₄]SnI ₄	1.963 X 10 ⁻⁷	8.625	10.597	1.79	S9
(1,4-BDA)SnI ₄	7.448 X 10 ⁻⁶ , 3.0043 X 10 ⁻⁶	3.3198, 3.1313	10.181	1.94	This work

^aOnly phases with crystallographic data are listed.

Table S2. Single crystal data and structure refinement details of (1,4-BDA)SnBr₆.

CCDC No.	2303742
Empirical formula	(1,4BDA)SnBr ₆
Formula weight	688.28
Temperature	273(2) K
Crystal system	Monoclinic
Space group	<i>P</i> 2 ₁ / <i>m</i>
Unit cell dimensions	a = 10.1731(4) Å α = 90° b = 7.5558(3) Å β = 99.2730(10)° c = 10.3974(4) Å γ = 90°
Volume	788.76(5) Å ³
Z	2
Density (calculated)	2.839 mg/m ³
Absorption coeff.	16.785 mm ⁻¹
θ range	2.028 to 27.107 °
Reflections collected	13694
Independent reflections	1876 [R(int) = 0.0784]
Data completeness	99.9 %
Data/restraints /parameters	1876 / 0 / 76
GoF on <i>F</i> ²	1.023
Final <i>R</i> indices [<i>I</i> > 2σ(<i>I</i>)]	<i>R</i> 1 = 0.0577, <i>wR</i> 2 = 0.1727
<i>R</i> indices (all data)	<i>R</i> 1 = 0.0680, <i>wR</i> 2 = 0.1844

Table S3. Single crystal data and structure refinement details of (1,4-BDA)SnBr₄.

CCDC No.	2303743
Empirical formula	(1,4BDA)SnBr ₄

Formula weight	528.48
Temperature	300(2) K
Crystal system	Monoclinic
Space group	<i>C</i> 2/c
Unit cell dimensions	a = 11.6179(5) Å α = 90° b = 11.8042(5) Å β = 100.415(2) ° c = 19.4177(8) Å γ = 90°
Volume	2619.07(19)Å ³
Z	8
Density (calculated)	2.681 mg/m ³
Absorption coeff.	14.113 mm ⁻¹
θ range	2.133 to 27.100 °
Reflections collected	21599
Independent reflections	2900 [R(int) = 0.1354]
Data completeness	100.0 %
Data/restraints /parameters	2900 / 0 / 104
GoF on <i>F</i> ²	0.970
Final <i>R</i> indices [<i>I</i> > 2σ(<i>I</i>)]	<i>R</i> 1 = 0.0432, <i>wR</i> 2 = 0.0654
<i>R</i> indices (all data)	<i>R</i> 1 = 0.0956, <i>wR</i> 2 = 0.0777

Table S4. Single crystal data and structure refinement details of (1,4-BDA)SnI₄.

CCDC No.	2303744
Empirical formula	(1,4BDA)SnI ₄
Formula weight	179.12
Temperature	299(2) K
Crystal system	Triclinic
Space group	$P\bar{1}$
Unit cell dimensions	$a = 8.4665(8) \text{ \AA}$ $\alpha = 77.434(3)^\circ$ $b = 8.8203(7) \text{ \AA}$ $\beta = 68.287(3)^\circ$ $c = 11.2697(10) \text{ \AA}$ $\gamma = 89.901(3)^\circ$.
Volume	760.26(12) \AA^3
Z	8
Density (calculated)	3.130 mg/m^3
Absorption coeff.	9.766 mm^{-1}
θ range	2.000 to 27.273 $^\circ$
Reflections collected	26535
Independent reflections	3404 [R(int) = 0.0931]
Data completeness	100.0 %
Data/restraints /parameters	3404 / 0 / 105
GoF on F^2	1.079
Final R indices [I > 2 σ (I)]	R1 = 0.0459, wR2 = 0.1288
R indices (all data)	R1 = 0.0611, wR2 = 0.1377

Table S5. Bond distances & bond angles as obtained from the SCXRD data of the compounds reported in this study. We have also included nonbonding N-H····X distances.

(1,4-BDA)SnBr₆	
<i>Bond lengths</i> (Å)	<i>Bond angles</i> (°)
Sn(1)-Br(1) = 2.6076(9) x 2 Sn(1)-Br(2) = 2.6252(15) Sn(1)-Br(3) = 2.5797(8) x 2 Sn(1)-Br(4) = 2.5989(13)	Br(4)-Sn(1)-Br(3) = 90.61(4) Br(3)-Sn(1)-Br(3) = 92.41(4) Br(1)-Sn(1)-Br(3) = 88.69(3) x 2 Br(1)-Sn(1)-Br(1) = 90.20(4) x 2 Br(2)-Sn(1)-Br(1) = 88.66(4) Br(2)-Sn(1)-Br(3) = 90.59(4) Br(4)-Sn(1)-Br(1) = 90.11(4) x 2
(1,4-BDA)SnBr₄	
<i>Bond lengths</i> (Å)	<i>Bond angles</i> (°)
Sn(1)-Br(1) = 2.7902(10) Sn(1)-Br(2) = 2.9752(6) Sn(1)-Br(3) = 3.1970(12) Sn(1)-Br(4) = 2.9808(6) Sn(1)-Br(5) = 3.3009(9) Sn(1)-Br(5) = 2.7426(9)	Br(5)-Sn(1)-Br(3) = 100.40(3) & 84.17(3) Br(5)-Sn(1)-Br(2) = 89.32(4) & 87.89(4) Br(5)-Sn(1)-Br(4) = 92.43(4) & 90.00(4) Br(5)-Sn(1)-Br(1) = 88.34(4) & 86.98(3) Br(4)-Sn(1)-Br(3) = 91.83(3) Br(3)-Sn(1)-Br(2) = 92.48(3) Br(1)-Sn(1)-Br(4) = 90.85(3) Br(1)-Sn(1)-Br(2) = 84.54(3)
<i>N-H····Br distances</i> (Å)	
N(1)-Br(1) = 3.418(8) N(1)-Br(3) = 3.366(8) N(1)-Br(5) = 3.605(9) N(2)-Br(1) = 3.446(6) N(2)-Br(2) = 3.497(6) N(2)-Br(3) = 3.373(6) N(2)-Br(5) = 3.591(7)	
(1,4-BDA)SnI₄	
<i>Bond lengths</i> (Å)	<i>Bond angles</i> (°)
Sn(1)-I(1) = 3.1439(7), 3.1440(7) Sn(1)-I(3) = 3.1641(6) Sn(1)-I(4) = 3.1596(6) Sn(2)-I(2) = 3.1485(7), 3.1486(7) Sn(2)-I(3) = 3.1610(6) Sn(2)-I(4) = 3.1592(6)	I(1)-Sn(1)-I(3) = 90.068(19) & 89.932(19) I(1)-Sn(1)-I(4) = 87.030(19) & 92.970(19) I(2)-Sn(2)-I(3) = 87.153(19) & 92.847(19) I(2)-Sn(2)-I(4) = 90.127(19) & 89.873(19)
<i>N-H····I distances</i> (Å)	
N(1)-I(1) = 3.675(11) N(1)-I(2) = 3.586(13) N(1)-I(3) = 3.658(10) N(2)-I(2) = 3.621(10) N(2)-I(4) = 3.694(12) N(2)-I(3) = 3.988(11)	

Bond length deviation (Δd) : It was calculated using the below formula:^{S10}

$$\Delta d = \frac{1}{6} \sum_i \left[\frac{d_i - d}{d} \right]^2$$

where d_i is the length of i^{th} M-X bond; d is the averaged M-X bond length.

Bond angle variance (σ^2) : It was calculated using the below formula:^{S11}

$$\sigma^2 = \sum_i \frac{1}{11} (\theta_i - 90)^2$$

where θ_i is the i^{th} X-M-X bond angle.

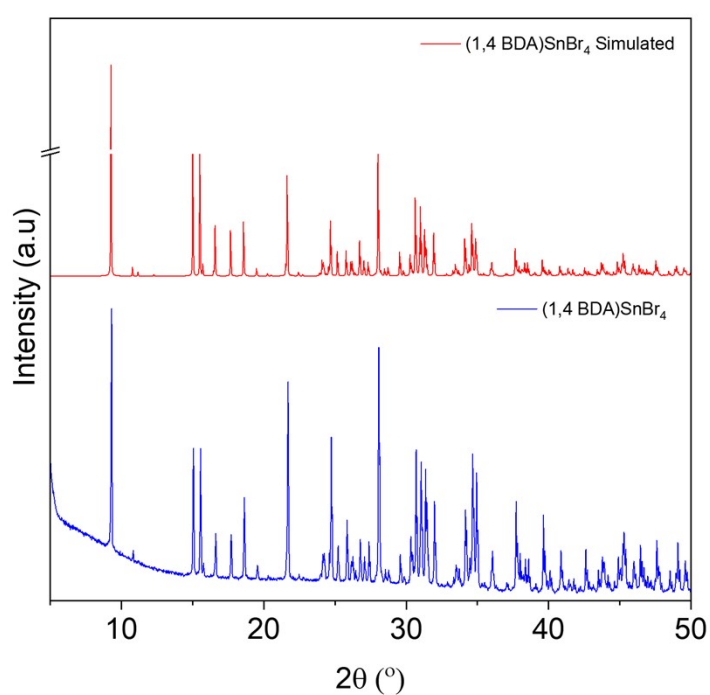


Fig. S1. Simulated and experimental powder X-ray diffraction patterns of (1,4-BDA)SnBr₄.

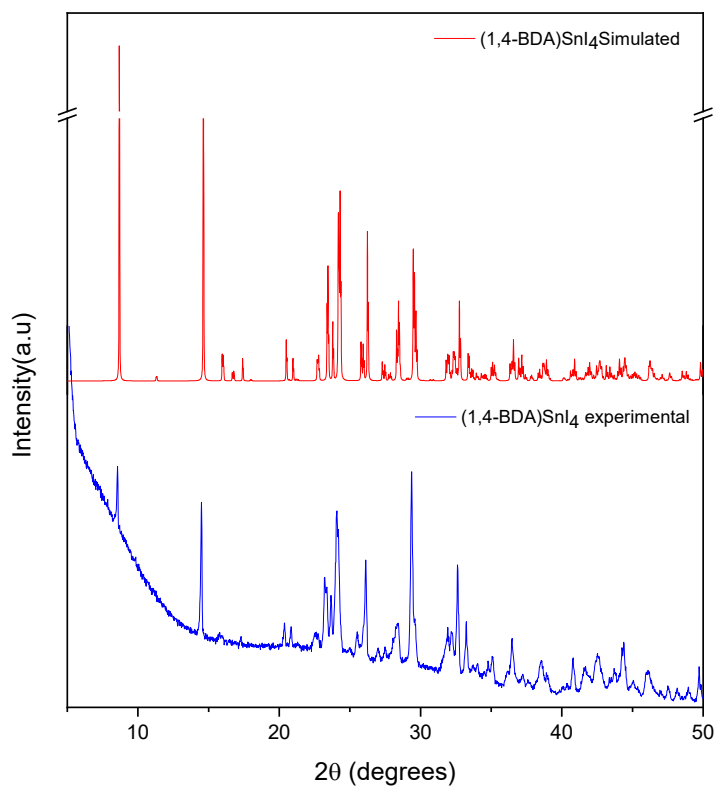


Fig. S2. Simulated and experimental powder X-ray diffraction patterns of (1,4-BDA)SnI₄.

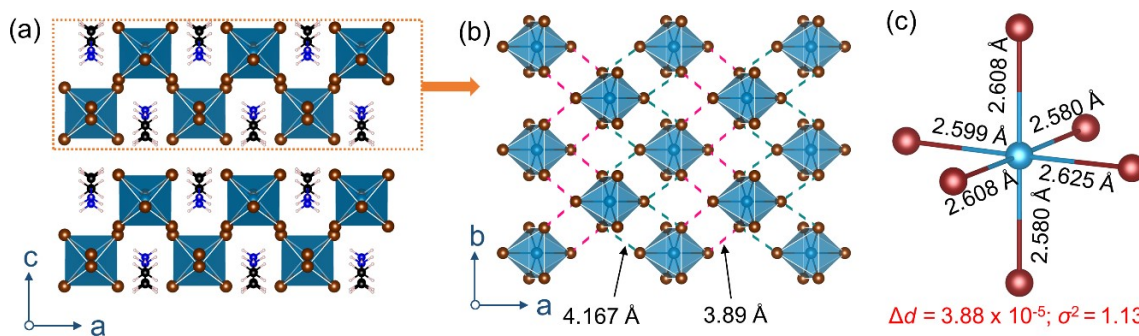


Fig. S3. Single-crystal structure of (1,4-BDA)SnBr₆: (a) Packing diagram viewed along the *b*-axis. (b) Arrangement of [SnBr₆]²⁻ octahedra in the *ab*-plane, showing the nearest neighbour Br···Br distance by green and red dashed lines (1,4-BDA) molecules are shown for sake of clarity). (c) An [SnBr₆]²⁻ octahedron showing the Sn-Br bond lengths (values for the bond length deviation & bond angle variance indices are also provided).

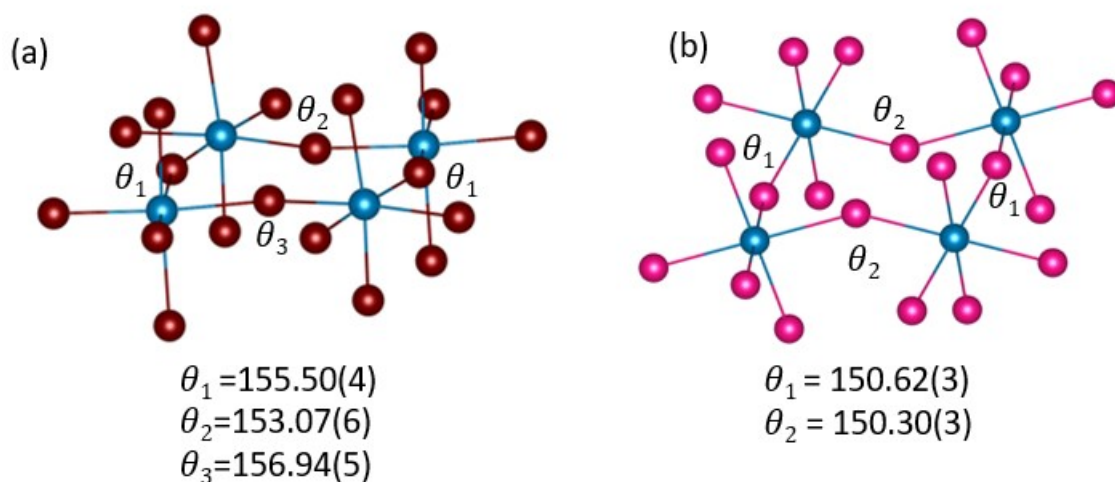


Fig. S4. (a) and (b) are Ball and Stick model of the perovskite layer illustrating the connection between the $(\text{SnBr}_6)^+$ and $(\text{SnI}_6)^+$ and corresponding M-X-M bond angles in (1,4-BDA) SnBr_4 and (1,4-BDA) SnI_4 respectively.

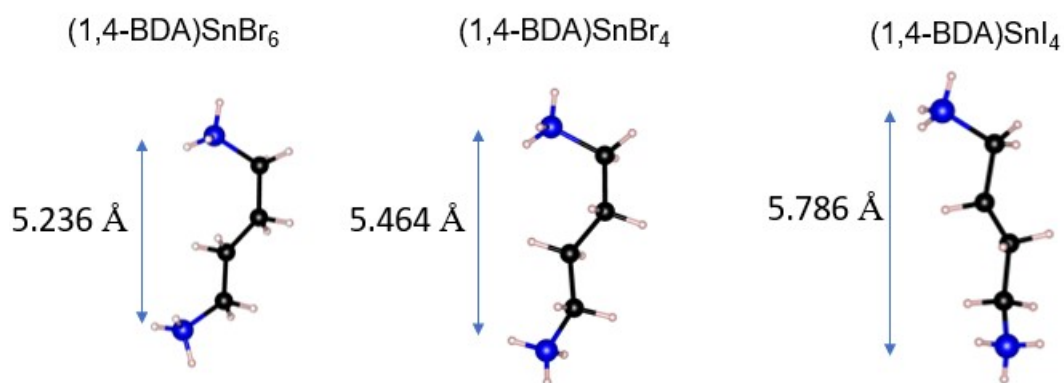


Fig. S5. Orientation of BDA in three different structures reported in this study, the distance between the NH_3^+ terminals are also given for comparison.

Table S6. Elemental ratio (atomic %) obtained from the EDS spectra.

Compound	C	N	Sn	Br	I
(1,4-BDA) SnBr_4	51.46	22.86	5.38	20.31	-
(1,4-BDA) SnI_4	67.70	7.43	5.33	-	19.54

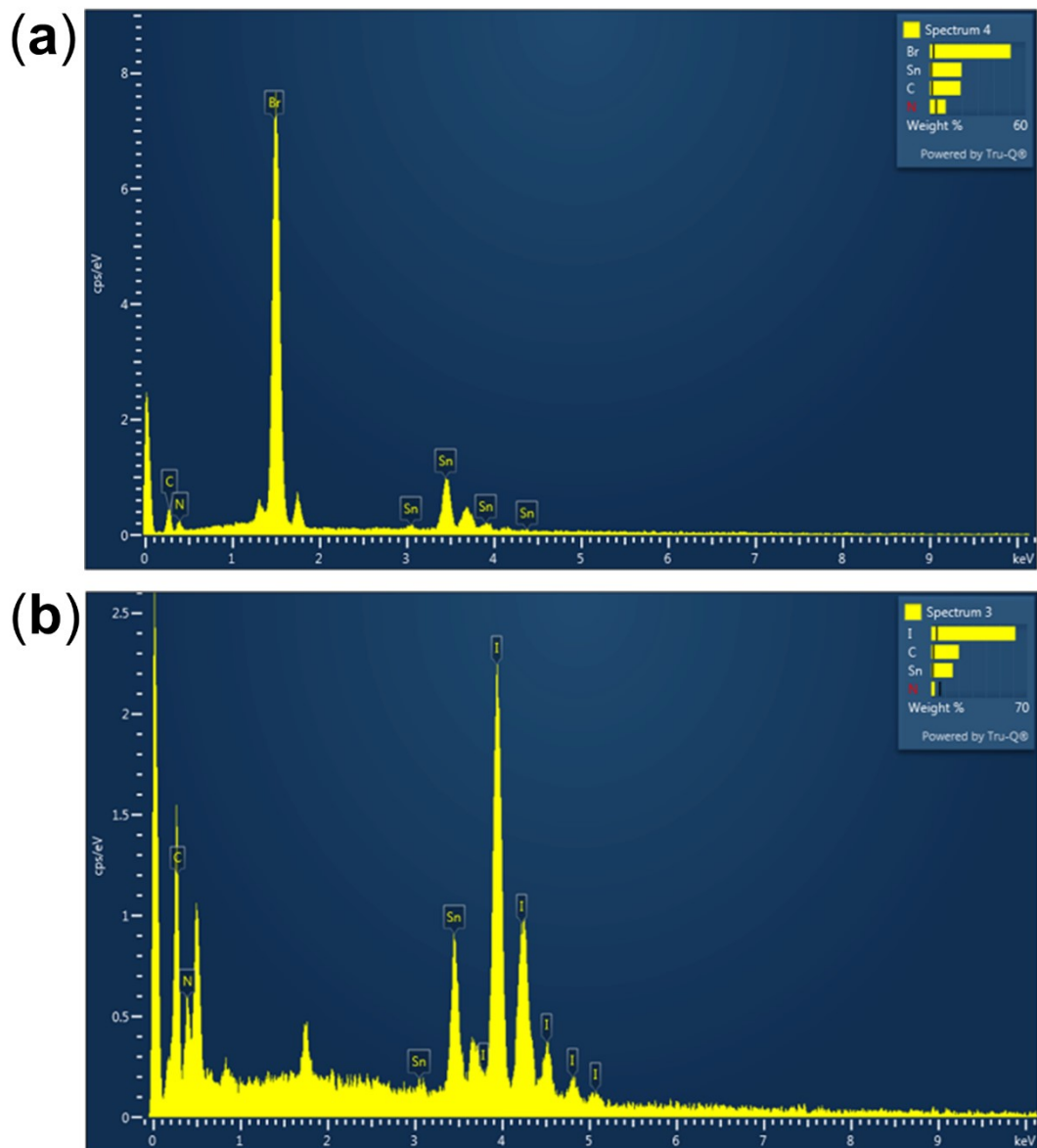


Fig. S6. Energy-dispersive X-ray spectra of (a) (1,4-BDA)SnBr₄ and (b) (1,4-BDA)SnI₄.

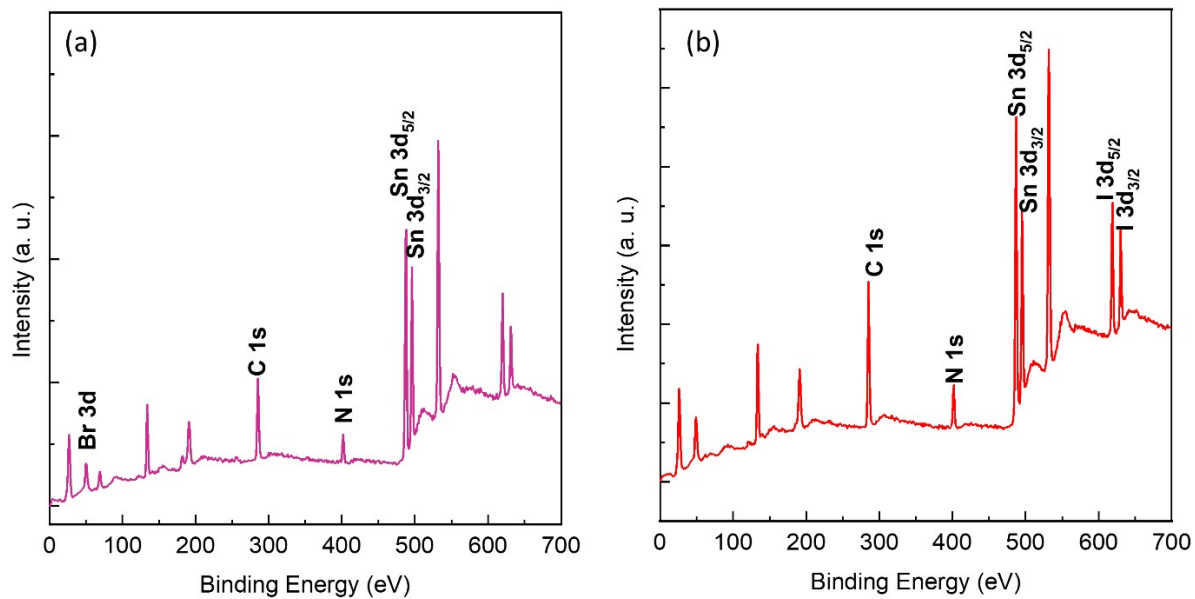


Fig. S7. XPS survey spectra of (a) (1,4-BDA)SnBr₄ and (b) (1,4-BDA)SnI₄.

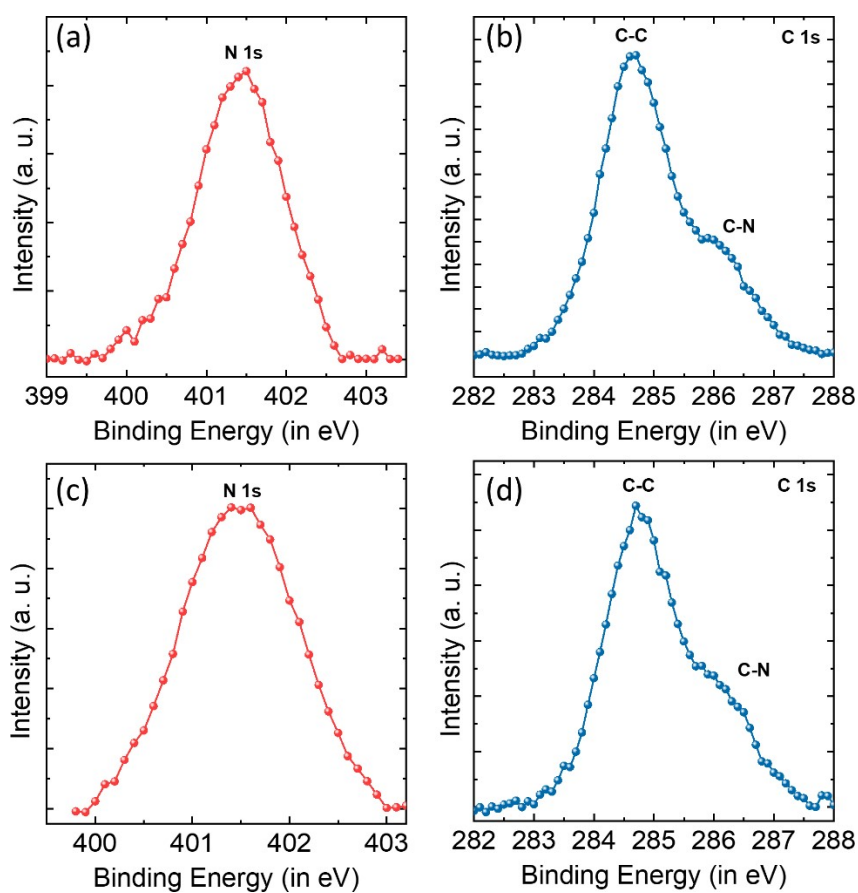


Fig. S8. (a) & (b) Core level N1s and C1s XPS spectra of (1,4-BDA)SnBr₄. (c) & (d) Core level N1s and C1s XPS spectra of (1,4-BDA)SnI₄.

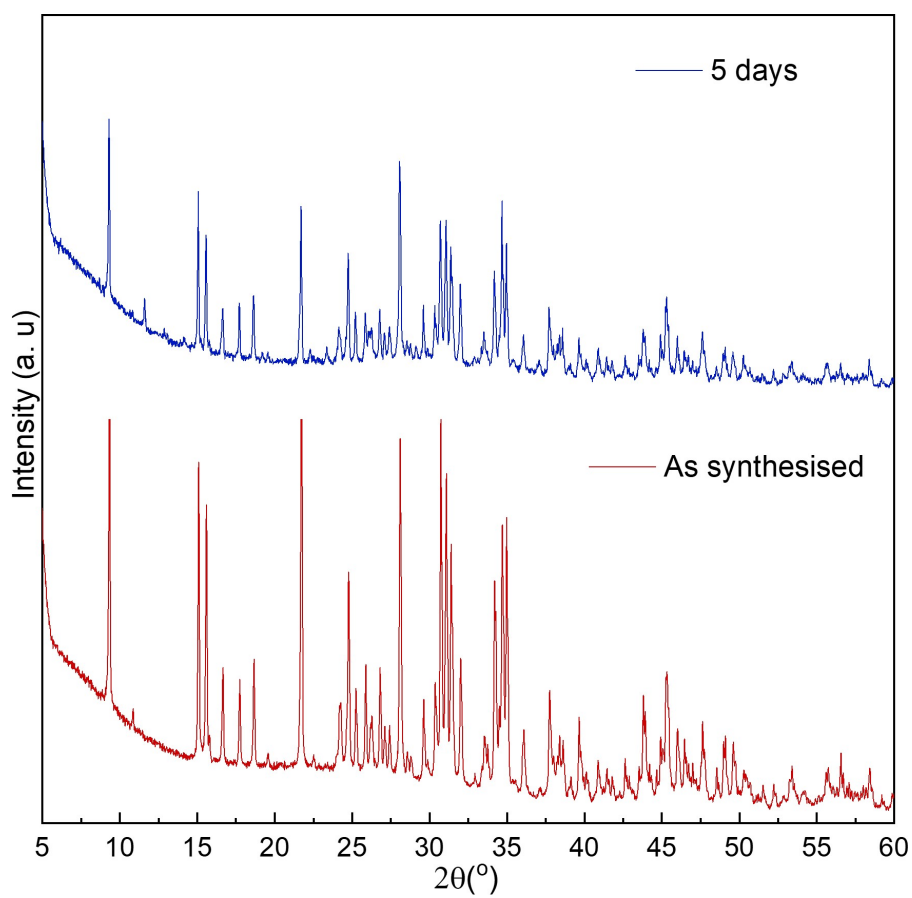


Fig. S9. PXRD pattern comparing the ambient stabilities of (1,4-BDA)SnBr₄.

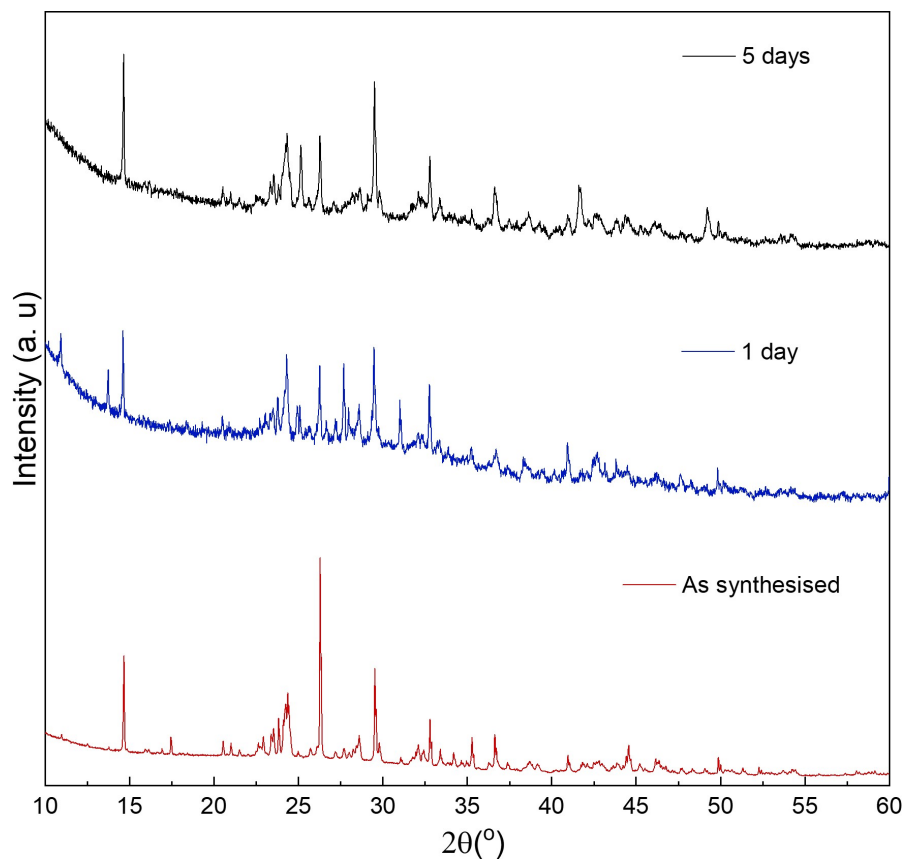


Fig. S10. PXRD pattern comparing the ambient stabilities of (1,4-BDA)SnI₄.

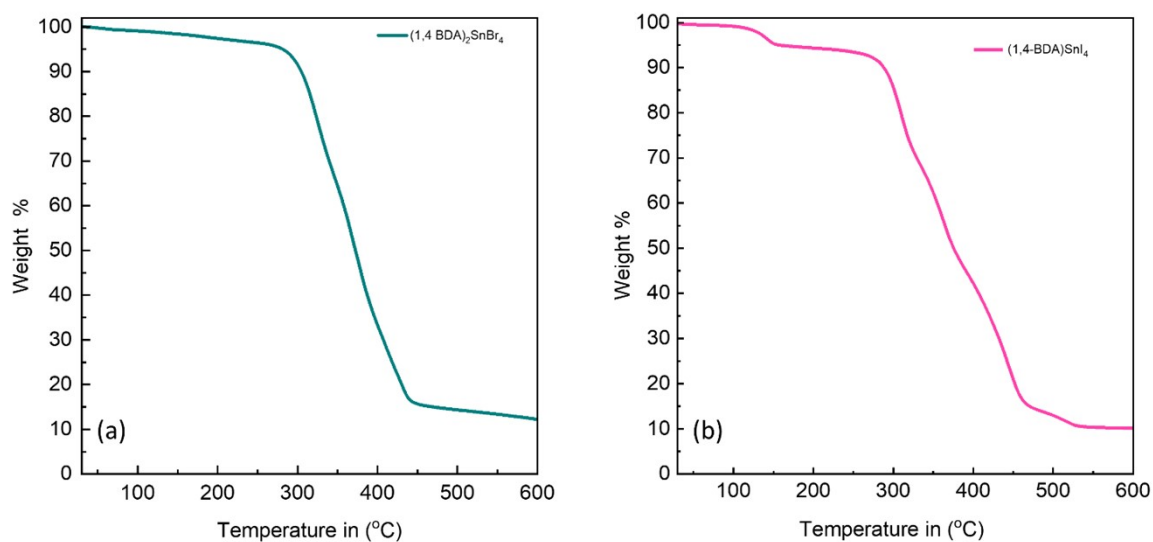


Fig. S11. TGA curves of (a) (1,4-BDA)SnBr₄ and (b) (1,4-BDA)SnI₄.

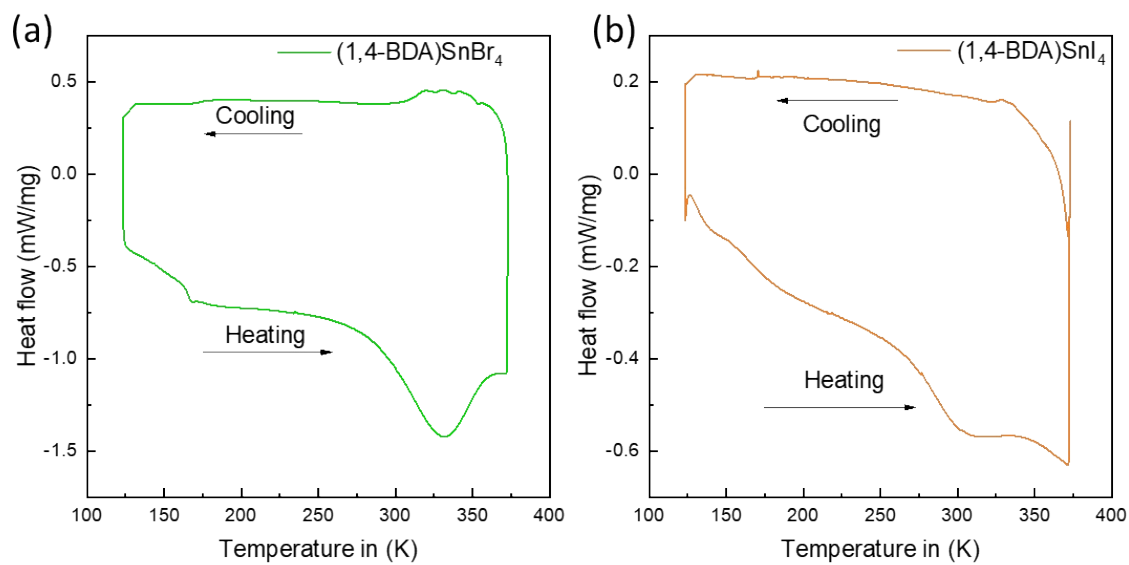


Figure S12. DSC plots of (a) (1,4-BDA)SnBr₄ and (b) (1,4-BDA)SnI₄.

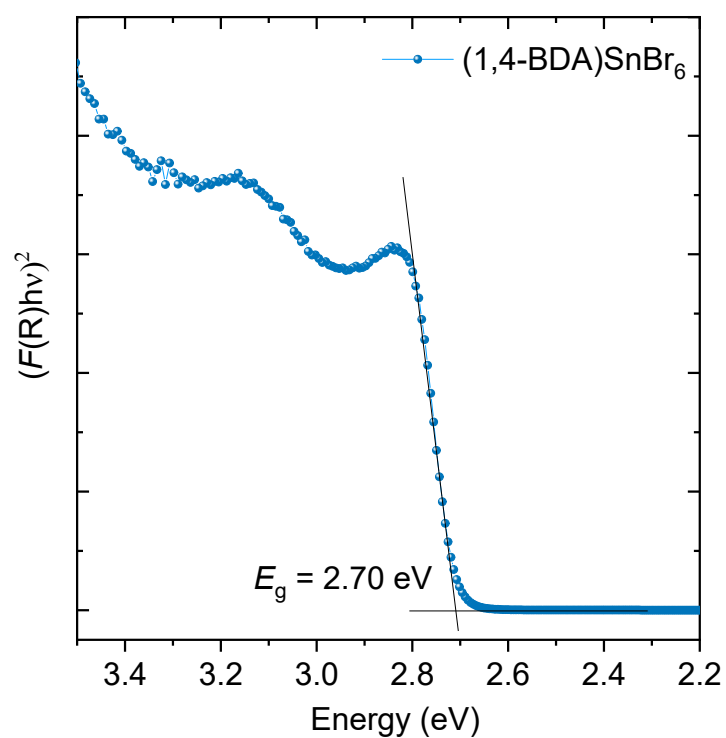


Fig. S13. Tauc plot for (1,4-BDA)SnBr₆.

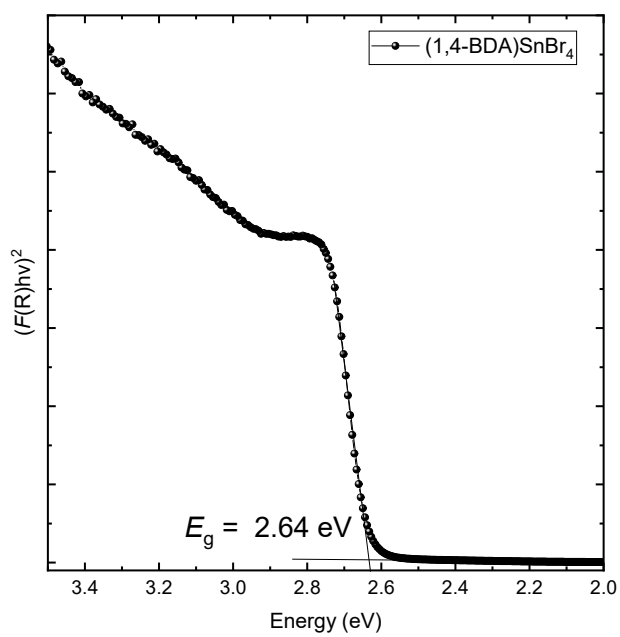


Fig. S14. Tauc plot for (1,4-BDA)SnBr₄.

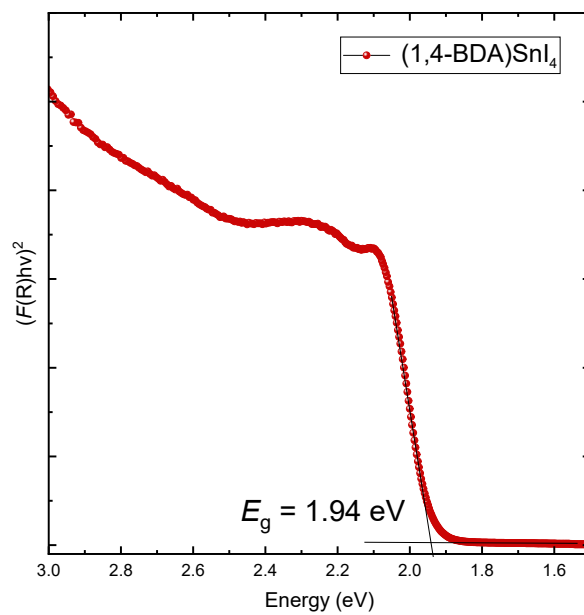


Fig. S15. Tauc plot of (1,4-BDA)SnI₄.

References

- S1 G. M. Sheldrick, *Acta Crystallogr. Sect. A Found. Adv.*, 2015, **71**, 3–8.
- S2 O. V. Dolomanov, L. J. Bourhis, R. J. Gildea, J. A. K. Howard and H. Puschmann, *J. Appl. Crystallogr.*, 2009, **42**, 339–341.
- S3 K. Momma and F. Izumi, *J. Appl. Crystallogr.*, 2011, **44**, 1272–1276.
- S4 S. Wang, J. Popović, S. Burazer, A. Portniagin, F. Liu, K.-H. Low, Z. Duan, Y. Li, Y. Xiong, Y. Zhu, S. V Kershaw, A. B. Djurišić and A. L. Rogach, *Adv. Funct. Mater.*, 2021, **31**, 2102182.
- S5 Y. Takahashi, R. Obara, K. Nakagawa, M. Nakano, J. Tokita and T. Inabe, *Chem. Mater.*, 2007, **19**, 6312–6316.
- S6 L. Mao, H. Tsai, W. Nie, L. Ma, J. Im, C. C. Stoumpos, C. D. Malliakas, F. Hao, M. R. Wasielewski, A. D. Mohite and M. G. Kanatzidis, *Chem. Mater.*, 2016, **28**, 7781–7792.
- S7 Z. Xu, D. B. Mitzi and D. R. Medeiros, *Inorg. Chem.*, 2003, **42**, 1400–1402.
- S8 Z. Tang, J. Guan and A. M. Guloy, *J. Mater. Chem.*, 2001, **11**, 479–482.
- S9 I. Zimmermann, S. Aghazada and M. K. Nazeeruddin, *Angew. Chem. Int. Ed.*, 2019, **58**, 1072–1076.
- S10 B. Sun, X.-F. Liu, X.-Y. Li, Y. Zhang, X. Shao, D. Yang and H.-L. Zhang, *Chem. Mater.*, 2020, **32**, 8914–8920.
- S11 K. Robinson, G. V Gibbs and P. H. Ribbe, *Science*, 1971, **172**, 567–570.